Nanoscale

Accepted Manuscript

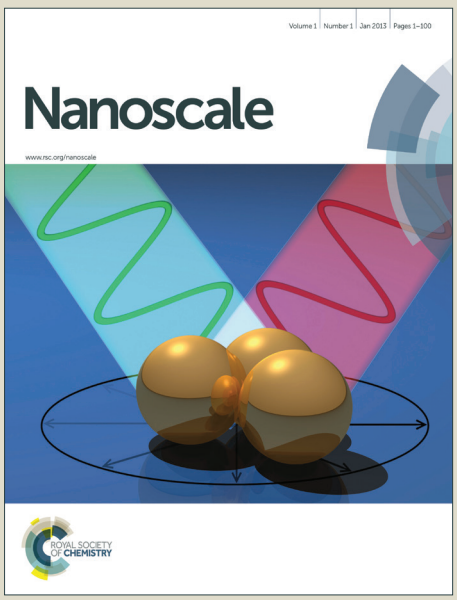

ROYAL SOCIETY OF CHEMISTRY

www.rsc.org/nanoscale

Anisotropic thermal conductivity of graphene wrinkles

C. Wang[1a], Y. Liu[a], L. Li[b], and H. Tan[a]

[a] *Center for Composite Materials, Harbin Institute of Technology, Harbin 150080, China*

[b] *Department of Materials Science and Engineering (MSE), KAUST-CU Center for Energy and Sustainability, Cornell University, Ithaca, NY, 14850, USA.*

Abstract:

In this paper, the anisotropic thermal conductivity characteristics of graphene wrinkles are observed for the first time using non-equilibrium molecular dynamics method. Our results reveal that the wrinkling level has little effect on the thermal conductivity along the wrinkling direction. However, the wrinkling level plays an important role in the reduction of thermal conductivity along the texture direction, which results from the contributions of increased bond length, Mises stress, broadening of phonon modes and G-band redshift. These results indicate that graphene wrinkles can be a promising candidate to modulate thermal conductivity properties in nanoscale thermal managements and thermoelectric devices.

1. Introduction

Single layer graphene sheet (SLGS), a two dimensional carbon atoms layer arranged in a honeycomb lattice with sp^2 bonds,[1] has become a focus of scientific research due to its various excellent properties, such as extraordinary thermal, electrical, optical, and mechanical properties, etc.[2-5] These outstanding properties extend the applications of graphene in nanomechanical systems, nanocomposites and electronic devices.[6-7] As several experiments have recently confirmed its superior thermal conductivity ranging from 2500-5300 W/mK,[8-9] the graphene is considered as the potential functional material in thermoelectrics and thermal

[1] Corresponding author. Tel/Fax: +86 0451 86402317. E-mail: wangcg@hit.edu.cn. C.G.Wang, Prof., Dr., Assistant director of CCMS HIT. AIAA member.

management, etc.[10-11] Meanwhile, many efforts have been explored to tune its thermal conductivity by defects,[12-13] tailored geometry,[14-16] impurity[17-18] and stress/strain[19-21] to meet the application requirements. Among all these methods, the wrinkle could be one of the most competitive candidates because of its easiness formation in graphene and continuous tunability at the nanoscale. The wrinkles may be formed and tuned by the inductivities of many ripples, chemical functional groups, defects, thermal or mechanical strains.[22-27] In addition, wrinkle has been demonstrated to be closely related to properties of graphene. However, using wrinkles as a technique to tune properties of graphene is still limited to the range of electronic transport and resonant frequencies of graphene.[28-29] Few studies were performed on the detailed influence of wrinkling and its corresponding mechanism of tuning the thermal properties of graphene.

In this paper, we perform non-equilibrium molecular dynamics to investigate the effect of shear-wrinkling on thermal conductivity of graphene. One wrinkling wave is then captured to emphatically analyze its pattern and directional effects on thermal conductivity. Finally, the physical insight of wrinkling effects on thermal conductivity is discussed and some prospective ideas about the design of excellent nanoscale thermal managements and thermoelectric devices are proposed.

2. Method and model

The thermal conductivities of SLGS are calculated using the non-equilibrium molecular dynamics (NEMD)[30]. The interaction potential between carbon atoms is described by AIREBO potential. The initial structure of a rectangular SLGS (67.5 Å×28.3 Å) with periodic boundary conditions is relaxed in canonical ensemble (NVT) ensemble at 300 K. After relaxing for 0.5 ns with a simulation time step of 0.5 fs, the system was then applied with a constant energy ensemble (NVE) condition in succession. The atoms in two length directions are fixed to prevent from sublimating. Hot and cold regions are then created in the simulation domain adjacent to the fixed boundary, by adding non-translational kinetic energy in the hot region and removing the same quantity from the cold region, respectively. The graphene with the thickness of 3.35 Å was used to calculate the cross-sectional area (A_C). The simulation sustained extra 5 ns to collect the spatial pattern of average established

temperature gradient, ($\partial T / \partial X$). The thermal conductivity (K) is then calculated using the Fourier law, as shown in the following, where q represents the heat flux in the graphene.

$$K = \frac{q}{A_c \cdot (\partial T / \partial X)} \quad (1)$$

3. Results and discussions

In order to calculate the thermal conductivity under different shear-wrinkling patterns, the shear strain is applied by shearing the left atom layer with 0.1 Å (shear strain 0.003). High shear strain increment means the increased numbers of shear-wrinkling patterns that SLGS can present. The graphene under strains will form three similar configurations which are the ripple, wrinkle and corrugation. The ripple is a necessary and natural condition which distributes randomly on graphene surface. It's a bulge slack configuration that the stress along the three directions is negligible. Another configuration likes a corrugation which is formed by axial or uniaxial compressive strains. pThe wrinkle is defined as a wave which goes across the whole graphene and has a distinct direction. It is tensioned greatly along wrinkling direction and compressed slightly along texture direction. Compared with the random ripples and corrugations, the characteristic parameters of wrinkles are regular and directional.

Two wrinkling parameters, namely the wrinkling amplitude and wrinkling wavelength, are defined to characterize the wrinkles. The wrinkling parameter represents a mean level of wrinkling characteristics, which can be expressed as $\eta = \frac{1}{n}\sum_{i=1}^{n}\eta_i$. Hence, the mean wrinkling amplitude (η_A) and the mean wrinkling wavelength (η_λ) can be calculated based on the configuration along the texture direction, as shown in Fig. 1. Meanwhile, the percentage ratio of mean wrinkling amplitude to the mean wrinkling wavelength, $\gamma = (\eta_A / \eta_\lambda) \times 100\%$, was defined to characterize the wrinkling level. Large γ changes mean high wrinkling level.

The spatial pattern of average temperature gradient along the SLGS and the thermal conductivity under 0.34 shear strain are also shown in Fig. 1. The thermal conductivity is 58.7 W/mK with γ =12.6%. This value is in the same order with the reported of initial graphene,[19, 31] and lower than those derived from the experimental measurements, which may

be explained by the finite size of the graphenes.[32-33]

Figure 2 shows the relative thermal conductivity and wrinkling level with respect to different shear-wrinkling patterns, where the relative thermal conductivity, namely K/K_0, is used to describe the change of thermal conductivity. Accompanied by the increasing shear strain, the wrinkling amplitude and the shrinking wrinkling wavelength are also increased, indicating the rising of wrinkling level. The thermal conductivity, however, does not decrease linearly with the increasing wrinkling level through the whole range. The downward trend of thermal conductivity is linear to the shear strain at the small wrinkling level (γ <10%). As a comparison, the change of thermal conductivity decreased more greatly in the range of high wrinkling level (γ >10%).

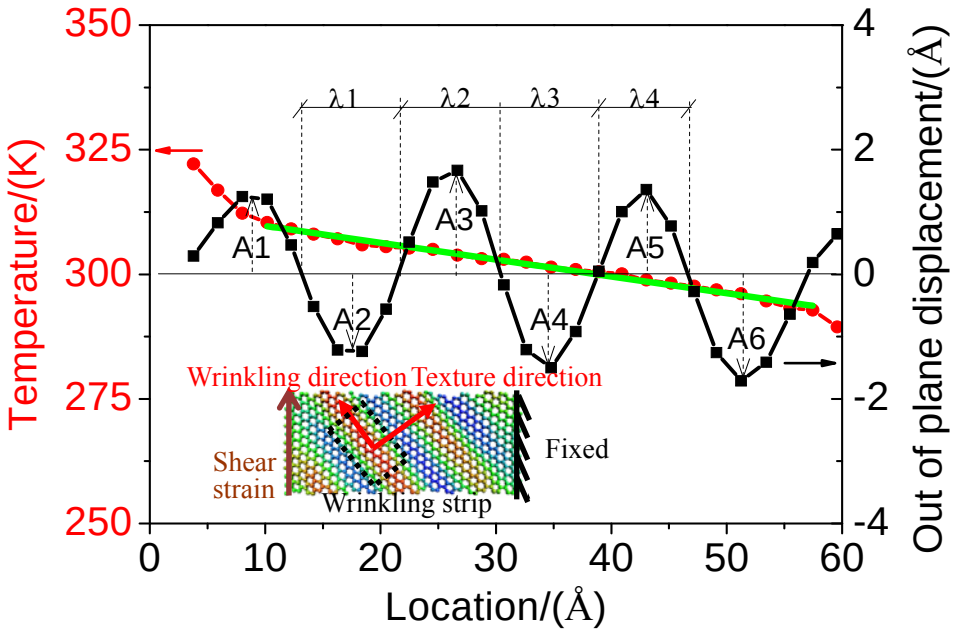

Fig.1 Wrinkling cross-section configuration, temperature gradient along texture direction and wrinkling model description (0.34 shear strain)

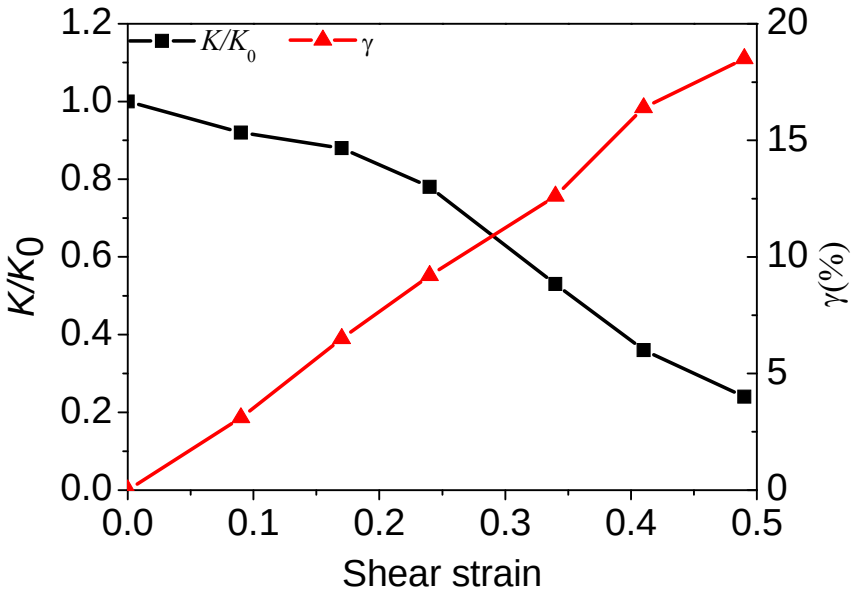

Fig.2 The relative thermal conductivity and wrinkling level under different shear strain

A specific wrinkling strip was then selected as an example to analyze the effect of wrinkles on thermal conductivity. In addition, the thermal conductivity along the wrinkling direction and texture direction respectively based on the wrinkling hyperbolic shape was calculated and presented in Fig. 3. It is interesting to observe the anisotropic thermal conductivity in a wrinkle. Specifically, the thermal conductivity along the texture direction decreases linearly at small wrinkling level. When γ is larger than 10%, the thermal conductivity decreases remarkably with a nonlinear trend. However, the wrinkling level has little influence (less than 6%) on the thermal conductivity along the wrinkling direction, which means the thermal conductivity along the wrinkling direction is nearly independent on the wrinkling level.

Based on above results, the wrinkled SLGS can be fabricated not to interact with the substrate and this will be favorable for reducing the thermal conduction in practice. This anisotropic characteristic indicates that the wrinkles can be tuned for different directions and levels to control the thermal conductivity properties of graphene in nanoscale thermal managements and thermoelectric devices. Next we design a device as a regulator of thermal conductivity using the anisotropic characteristics of wrinkles, which is shown in Fig. 4. We can switch on the thermal conductivity by tuning wrinkling direction parallel to that of heat flux, as plotted in Fig. 4 (a). Meanwhile, we can also block the thermal conductivity by designing wrinkling direction perpendicular to that of heat flux, as plotted in Fig. 4 (b). In a

word, we can tune the wrinkles to realize the thermal conductivity reduction within 80% range of initial graphene.

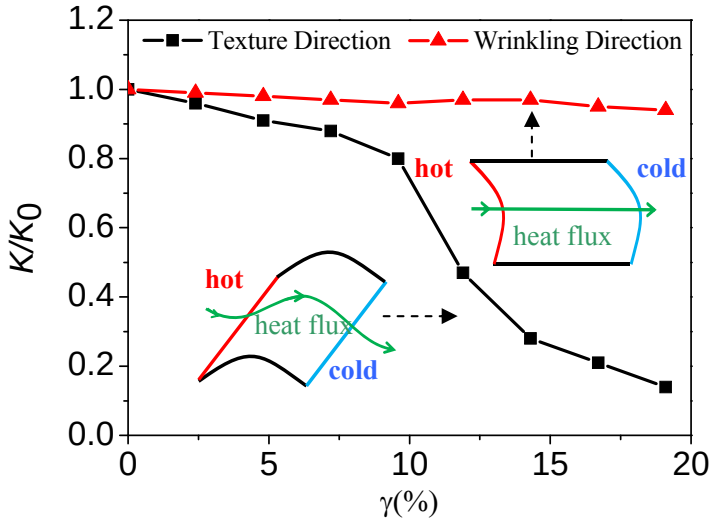

Fig.3 The relative thermal conductivity along the texture and wrinkling directions under different wrinkling level

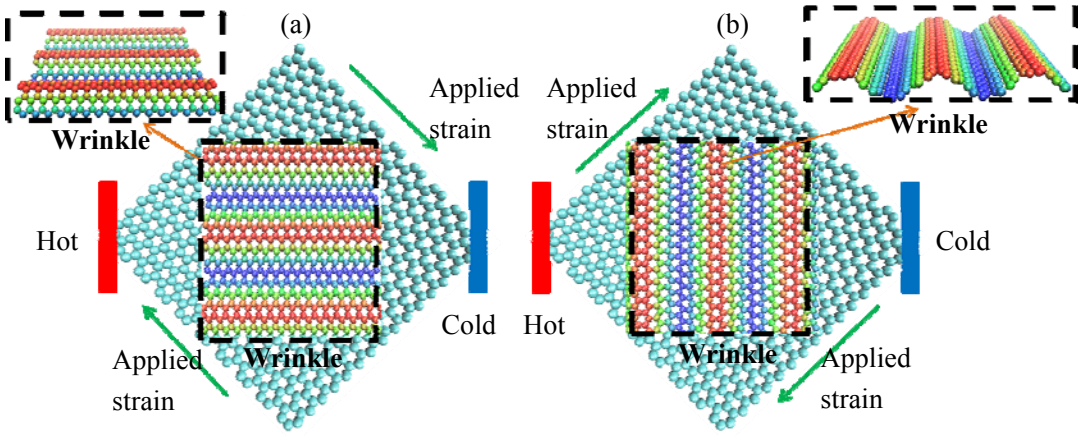

Fig.4 A thermal regulator design based on the graphene wrinkles (a) switch on the thermal conductivity (b) block the thermal conductivity

The radial distribution function (RDF) and mechanical properties are then used to explore the atomic structure change in the wrinkling strip, in order to further reveal the relationship between the wrinkled deformation and thermal conductivity. Notice that the mean C-C bond length is elongated from 1.428 Å to 1.456 Å with the increasing wrinkling level, as listed in Tab. 1. Therefore, the interactions among carbon atoms are weakened and a significant phonon softening can be expected to the reduction of thermal conductivity.

Tab.1 Mises stress and mean bond length of the wrinkling strip under different wrinkling level

wrinkling level(%)	Mises stress of atoms(MPa)	mean bond length(Å)
0	40.7	1.428
2.4	47.4	1.432
7.2	79.2	1.443
11.9	87.2	1.450
14.3	101.6	1.456

By analyzing the stress state of wrinkles, the wrinkles are tensioned along wrinkling direction and compressed along texture direction. In addition, the stretching stress is far from the compressive stress, which is big different from the other two configurations. For the wrinkles, the stress distribution is much more localized around the peak or the valley of wrinkles because of the formation of wrinkles. The Mises stress, σ_M, is introduced to evaluate the stress level of overall structures and expressed in the following equation (2):

$$\sigma_M = \sqrt{\left(\sigma_x - \sigma_y\right)^2 + \left(\sigma_y - \sigma_z\right)^2 + \left(\sigma_z - \sigma_x\right)^2 + 6\left(\tau_{xy} + \tau_{yz} + \tau_{xz}\right)^2} \quad (2)$$

where σ_x, σ_y and σ_z are the normal stress along the three directions, τ_{xy}, τ_{yz} and τ_{xz} are the shear stress in three planes respectively. According to Tab. 1, it can be noticed that the Mises stress ranges from 40.7 MPa to 101.6 MPa and the stress concentrates around the wrinkling peak corresponding to the increasing wrinkling level. A large stress gradient ranging from 23.2 MPa to 40.3 MPa can be observed apparently for the specific texture direction when the wrinkling level reaches 11.9%, as is shown in Fig. 5. This large stress gradient results in the increase of phonon scattering and thus reduces the thermal conductivity to 47% of the pristine graphene. In contrast to the texture direction, the stress gradient (2.6 MPa) is unconspicuous along wrinkling direction. Furthermore, the stress increment along the wrinkling direction changes little with the increase of wrinkling level, indicating wrinkles have negligible influences on phonon scattering along wrinkling direction. Therefore, the thermal conductivity decreases no more than 6% along the wrinkling direction corresponding to an increasing wrinkling level.

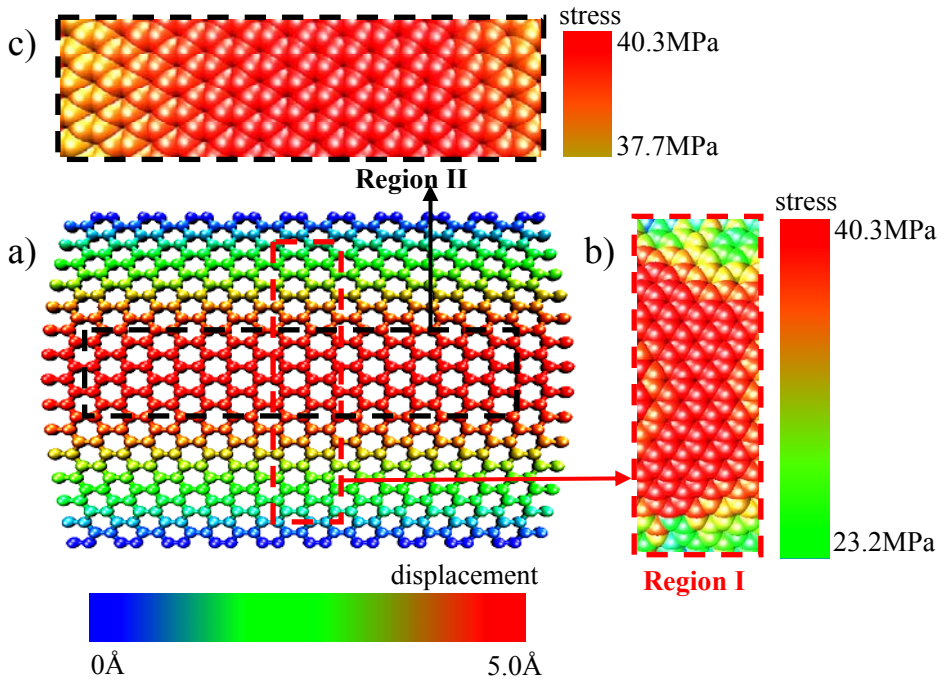

Fig.5 Mises stress and out-of-plane displacement distributions in wrinkling strip (γ=11.9%) (a) out-of-plane displacement distributions in wrinkling strip; (b) Mises stress of region I in wrinkling strip; (c) Mises stress of region II in wrinkling strip

In addition, different from pure strain, wrinkles have dual effects on thermal conductivity. Both the configuration and strain of wrinkles decide the thermal conductivity rather than strains alone. Configuration of wrinkles changes 2D atomic monolayer structure to 3D configuration and gives much stronger phonon scattering along out-of plane direction. Meanwhile strains result in the softening of the phonon modes and lead to the reduction of thermal conductivity.

The phonon density of states (DOS) evolution versus the wrinkling level, using the code Fix-Phonon,[34] is plotted in Fig. 6 to further understand the thermal conductivity reduction trend. It can be observed from Fig.6 (a) that the reduction of thermal conductivity can be attributed to two factors. Firstly, the redshift of G-band with respect to its wrinkling level is estimated. The results show that the G-band redshift ranges from 45.4 THz to 38.7 THz when the wrinkling level increases from 0 to 14.3%, indicating that the increasing wrinkles would soften the G-band of the phonon spectra which leads to the decrease of the phonon group velocities and reduction of thermal conductivity.[19] Secondly, the phonon mode peaks related to the heavy wrinkling level around 16 THz are broadened when γ is larger than 10%.

Especially, the valley curves are gradually flattened by broadening of adjacent peaks when the wrinkling level increases. The phonon lifetime can be expressed as $\tau = 0.5l^{-1}$, where τ is the lifetime and l is the half-width at half-maximum.[35] Therefore, the broadening of the phonon modes indicates the reduction of the phonon lifetime and leads to the decrease of thermal conductivity. This is attributed to the decreased lifetime of the corresponding modes. The broad peaks in DOS may also be explained as an indication of phonon scattering due to the stress concentration around the wrinkling peaks. Meanwhile, an apparent increase of DOS value below 13 THz leads to more phonon scattering[36] and results in a further reduction of thermal conductivity at high wrinkling levels (γ>10%). This may explain why a more apparent thermal conductivity reduction in Fig. 3 is observed for the range with wrinkling level larger than 10%.

In addition, compared with the phonon DOS along texture direction, there is no obvious broadening of the phonon modes along wrinkling direction, which is shown in Fig. 6 (b). Meanwhile, the decrement of G-band frequency is only 1.24 THz, which is far smaller than 6.59 THz in Fig. 6 (a). Therefore, the redshift of G-band phonon frequency has a small relationship with the heavy wrinkling level along the wrinkling direction. And it is the reason that the thermal conductivity along the wrinkling direction is nearly independent on the wrinkling level.

(a)

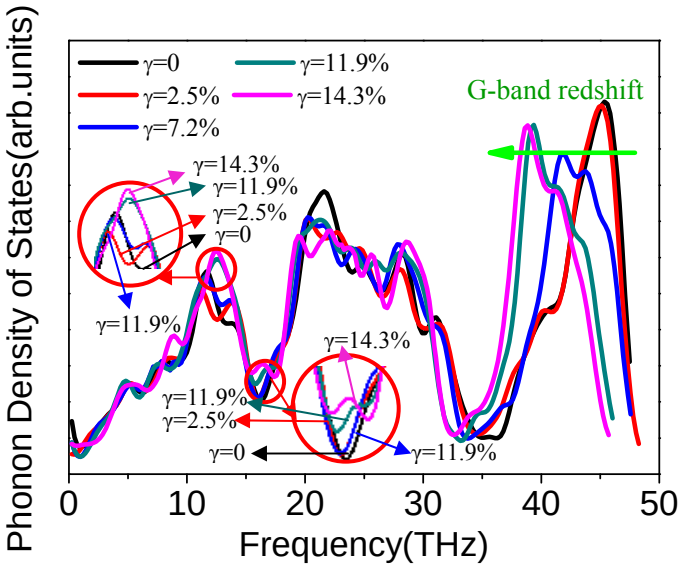

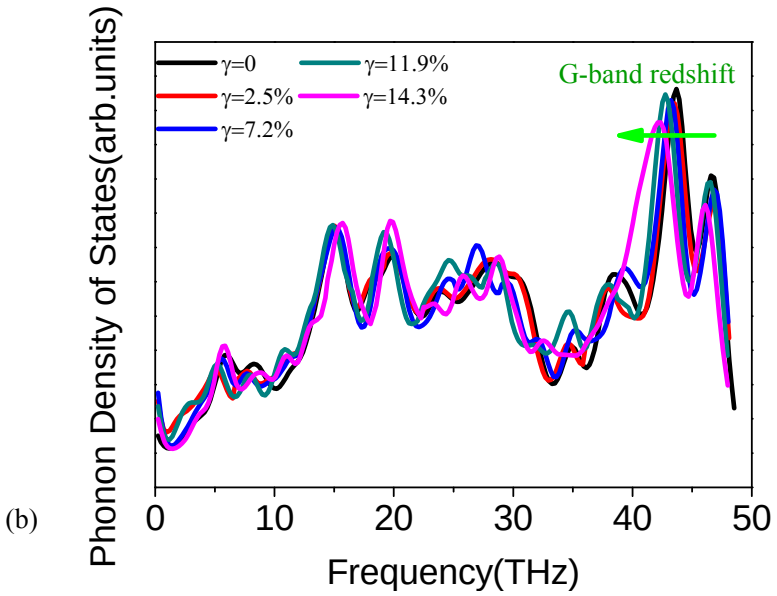

Fig.6 Phonon DOS analysis on the effect of wrinkling level (a) along the texture direction; (b) along the wrinkling direction

4. Conclusions

To sum up, the wrinkle plays an active role in the anisotropic thermal conductivity of graphene. The thermal conductivity of graphene may be tuned by wrinkling level or direction to achieve 80% reduction compared with the initial graphene. Meanwhile, the wrinkling direction can also be used to avoid the interaction between the graphene and the substrate to maintain the thermal conductivity in practice. The reduction of thermal conductivity is related to the mean bond length elongation, stress gradient increment and G-band redshift for the slightly wrinkled graphene. The heavily wrinkled graphene shows a dramatic reduction on the thermal conductivity, which is attributed to the broadening phonon modes and an apparent increase of DOS value. The anisotropic characteristic of wrinkle shown in this paper confirms that graphene wrinkles can be tuned for different directions and levels to control the thermal conductivity properties in nanoscale thermal managements and thermoelectric devices.

Acknowledgements

Authors would like to thank Prof. Gang Zhang (Peking University) for his help in simulation. Authors gratefully acknowledge supports from National Natural Science Foundation of China, 11172079; Program for New Century Excellent Talents in University, NCET-11-0807; the Fundamental Research Funds for the Central Universities,

HIT.BRETIII.201209 and HIT.NSRIF.201156.

References

1 A. K. Geim, K. S. Novoselov, *Nat. Mater.*, 2007, **6**, 183.

2 C. Lee, X. Wei, J. W. Kysar, J. Hone, *Science*, 2008, **321**, 385.

3 Y. B. Zhang, Y. W. Tan, H. L. Stormer, P. Kim, *Nature*, 2005, **438**, 201.

4 P. Avouris, *Nano Lett.*, 2010, **10**, 4285.

5 A. A. Balandin, *Nature Mater.*, 2011, **10**, 569.

6 J. S. Bunch, A. M. van der Zande, S. S. Verbridge, I. W. Frank, D. M. Tanenbaum, J. M. Parpia, et al., *Science*, 2007, **315**, 490.

7 K. Kordas, G. Toth, P. Moilanen, M. Kumpumaki, J. Vahakangas, A. Uusimaki, R. Vajtai and P. M. Ajayan, *Appl. Phys. Lett.*, 2007, **90**, 123105.

8 S. Ghosh, I. Calizo, D. Teweldebrhan, E. P. Pokatilov, D. L. Nika, A. A. Balandin, et al., *Appl. Phys. Lett.*, 2008, **92**, 151911.

9 A. A. Balandin, S. Ghosh, W. Z. Bao, Calizo I, Teweldebrhan D, F. Miao, et al., *Nano Lett.*, 2008, **8**, 902.

10 J. Q. He, A. Gurguen, J. R. Sootsman, J. C. Zheng, L. Wu, Y. Zhu, M. G. Kanatzidis and V. P. Dravid, *J. Am. Chem. Soc.*, 2009, **131**, 17828.

11 J. N. Hu, X. L. Ruan and Y. P. Chen, *Nano Lett.*, 2009, **9**, 2730.

12 T. Y. Ng, J.J. Yeo, Z.S. Liu, *Carbon*, 2012, **50**, 4887.

13 F. Hao, D. N. Fang, and Z. P. Xu, *Appl. Phys. Lett.*, 2011, **99**, 041901.

14 N. Yang, X. X. Ni, J. W. Jiang, and B. W. Li, *Appl. Phys. Lett.*, 2012, **100**, 093107.

15 J. C. Zhang, X. W. Wang, *Nanoscale*, 2013, **5**, 734.

16 C. X. Yu, and G. Zhang, *J. Appl. Phys.*, 2013, **113**, 044306.

17 W. X. Huang, Q. X. Pei, Z. S. Liu, Y. W. Zhang, *Chem. Phys. Lett.*, 2012, **552** , 97.

18 Q. X. Pei, Y. W. Zhang, Z. D. Sha, and V. B. Shenov, *Appl. Phys. Lett.*, 2012, **100**, 101901.

19 N. Wei, L. Q. Xu, H. Q. Wang, and J. C. Zheng, *Nanotechnology*, 2011, **22**, 105705.

20 F. Ma, H. B. Zheng, Y. J. Sun, D. Yang, K. W. Xu, et al., *Appl. Phys. Lett.*, 2012, **101**, 111904.

21 X. B. Li, K. Maute, M. L. Dunn, and R. G. Yang, *Phys. Rev. B*, 2010, 81, 245318.

22 A. Fasolino, J. H. Los, and M. I. Katsnelson, *Nat. Mater.*, 2007, **6**, 858.

23 Q. Wu, Y. Wu, Y. Hao, J. Geng, M. Charlton, S. Chen, et al., *Chem. Commun.*, 2013, **49**, 677.

24 C. G. Wang, L. Lan, and H. F. Tan, *Phys.Chem. Chem. Phys.*, 2013, **15**, 2764.

25 K. Min and N. R. Aluru, *Appl. Phys. Lett.*, 2011, **98**, 013113.

26 C. G. Wang, Y. P. Liu, L. Lan, and H. F. Tan, *Nanoscale*, 2013, **5**, 4454.

27 W. H. Duan, K. Gong, and Q. Wang, *Carbon*, 2011, **49**, 3107.

28 Y. F. Guo, and W. L. Guo, *J. Phys. Chem. C*, 2013, **117**, 692.

29 C. G. Wang, L. Lan, Y. P. Liu, H. F. Tan, *Comp. Mater. Sci.*, 2013, **77**, 250.

30 P. Jund, and R. Jullien, *Phys. Rev. B*, 1999, **59**, 13707.

31 T. H. Liu, C. W. Pao, C. C. Chang, *Comp. Mat. Sci.*, 2013, **70**, 163.

32 A. Bagri, S. P. Kim, R. S. Ruoff, et al., *Nano Lett.*, 2011, **11**, 3917.

33 Z. Q. Wang, R. G. Xie, C. T. Bui, et al., *Nano Lett.*, 2011, **11**, 113.

34 L.T. Kong, Comp. *Phys. Commun.*, 2011, **182** , 2201.

35 J. A. Thomas, J. E. Turney, R. M. Iutzi, et al., *Phys. Rev. B*, 2010, **81**, 081411.

36 D. L. Nika, E. P. Pokatilov, A. S. Askerov, A. A. Balandin, Phys. Rev. B, 2009, **79**, 155413.